

Reliable *ab initio* calculation of a chemical reaction rate and a kinetic isotope effect: $\text{H} + \text{H}_2$ and ${}^2\text{H} + {}^2\text{H}_2$

(transition-state theory/tunneling/*ortho-para* hydrogen conversion/chemical dynamics)

BRUCE C. GARRETT AND DONALD G. TRUHLAR

Department of Chemistry, University of Minnesota, Minneapolis, Minnesota 55455

Communicated by Bryce Crawford, Jr., July 11, 1979

ABSTRACT We calculate equilibrium rate constants for *ortho-para* conversion in hydrogen and deuterium by an atomic mechanism. The calculations are based on an accurate *ab initio* potential surface, transition state theory, and an adiabatic transmission coefficient. The calculated rate constants are demonstrated to be reliable within 40–50%, and they agree with experiment within this margin.

The calculation of absolute reaction rates is an important goal of quantum chemistry. In this article we report calculations of the equilibrium rate constant and kinetic isotope effect for the gas-phase reaction



These calculations take advantage of several recent advances (1–9) in the theory and computation of chemical reaction rates from first principles—i.e., with no semiempirical elements. The procedures used have been carefully tested and the methods used are shown to be reliable to within about 40–50%, which is as good as or better than the experimental accuracy attainable for most reactions. There has been no previous completely *ab initio* calculation of a chemical reaction rate with this level of demonstrated reliability.

Theory

We use transition-state theory (refs. 10–12; recently reviewed in ref. 13). The difficulties in using this theory to predict absolute reaction rates fall into two categories. The first general obstacle is the lack of accurate information about potential energy hypersurfaces. For the $\text{H} + \text{H}_2$ reaction and isotopic analogs this obstacle has been largely overcome by the accurate *ab initio* configuration-mixing calculations of Liu and Siegbahn (3, 4). For the present calculations we use an accurate analytic representation of their calculated potential energy hypersurface (14). The error in using this surface is estimated by comparing to calculations on another surface that differs by a reasonable estimate of the basis-set truncation error in the configuration-mixing calculations. The second obstacle is the calculation of the transmission coefficient of conventional transition-state theory. This represents the deviation of the true equilibrium rate from that calculated with the conventional transition-state assumptions. The fundamental assumption is that all phase points on a configuration-space hypersurface (called the dividing surface) located at the saddle point of the potential energy surface cross the dividing surface only once. It is also assumed that a separable reaction coordinate exists, that the remaining degrees of freedom can be quantized in the usual way, and that motion along the reaction coordinate is classical. For $\text{H} + \text{H}_2$, the last assumption, classical reaction-coordinate

motion, is the one requiring the largest corrections, and we use Marcus and Coltrin's (7) variationally motivated collinear tunneling path (7) and a vibrationally adiabatic barrier, including bending contributions, to estimate quantum mechanical tunneling and nonclassical reflection in the reaction-coordinate motion. Another important aspect of the present calculation which is often missing in applications of transition-state theory is careful attention to anharmonicity (8, 9). The techniques used for the dynamics part of the calculation are tested by applying them to a Porter–Karplus potential energy surface for which accurate quantum mechanical close coupling calculations have been performed by Schatz and Kuppermann (5).

Computations and testing reliability of the results

The transition-state theory rate constant, in which all atoms are treated as distinguishable, is (9–12)

$$k^\ddagger(T) = \kappa(T) \sigma \frac{k_B T}{h} \frac{Q^\ddagger(T)}{\Phi^R(T)} \exp(-V^\ddagger/k_B T), \quad [2]$$

in which $\kappa(T)$ is the transmission coefficient, σ is a statistical symmetry factor, k_B is Boltzmann's constant, T is temperature, h is Planck's constant, $Q^\ddagger(T)$ is the transition-state partition function, $\Phi^R(T)$ is the reactant's partition function per unit volume, and V^\ddagger is the potential energy at the saddle point. The partition functions are evaluated as explained in detail in ref. 9. In particular, translation, stretching vibrations, rotation, and bending vibrations are assumed separable from each other, Morse anharmonicity is included in stretching vibrations, and quartic anharmonicity is included in bending vibrations. All harmonic and anharmonic force constants are evaluated directly from the potential energy surface.

The assumption that bends and rotations are separable at the saddle point can be questioned. It is hard to estimate the effect of bend-rotation coupling on the quantized energy levels, but a classical treatment (8) by the method of Strauss and Thiele (15) decreases the transition-state partition function for reaction 1 for the surface of ref. 14 by only 5–8% for 300–600 K as compared to a classical treatment using the quadratic-quartic separable approximation used here. Because classical mechanics is not valid at these temperatures and because the effect is small, we did not include this correction.

The transmission coefficient is evaluated as follows. We use a vibrationally adiabatic model for the transmission coefficient because, as emphasized elsewhere (16), this is the most consistent with the assumptions of transition-state theory. The minimum-energy path and Marcus–Coltrin tunneling path for a collinear collision are defined and determined from the potential energy surface as in ref. 7. Distances from the symmetric stretch line along these paths are called s and ξ , respectively, where ξ can be considered a function of s and of relative translational energy E_{rel} (somewhat confusingly, both s and ξ are called s in ref. 7). All along the minimum-energy path we compute the zero-point energy for the bound stretching vi-

The publication costs of this article were defrayed in part by page charge payment. This article must therefore be hereby marked "advertisement" in accordance with 18 U. S. C. §1734 solely to indicate this fact.

bration and the doubly degenerate bending vibration. For this calculation we include Morse anharmonicity for the stretch and quartic anharmonicity for the bend. Notice that in the reactant and product regions the stretching vibration becomes the H₂ vibration and the bending zero-point energy vanishes. For a given s and E_{rel} , and hence a given ξ , the sum $V_a^G(\xi, E_{\text{rel}})$ of the classical potential energy along the minimum-energy path and the local zero-point energy defines the ground-state, s -wave vibrationally adiabatic barrier

$$V^{\text{MCPVAG}}(\xi, E_{\text{rel}}) = V_a^G(\xi, E_{\text{rel}}) - V_a^G(\xi = -\infty, E_{\text{rel}}). \quad [3]$$

The abbreviation MCPVAG denotes "Marcus-Coltrin path, vibrationally adiabatic ground" state. The justification for the tunneling path for collinear collisions is given elsewhere (6) and will not be repeated here. We note, however, that the present treatment differs from that for a collinear collision in that the effective barrier is higher because some energy gets tied up in bending degrees of freedom. The quantum mechanical transmission probability $P(E_{\text{rel}})$ for the barrier $V^{\text{MCPVAG}}(\xi, E_{\text{rel}})$ is computed numerically (16) for a sequence of E_{rel} values and the results are numerically thermally averaged. The numerical uncertainties in the quantum transmission probabilities and averaging are kept less than 1%. The transmission coefficient is defined as the ratio of this average to the thermally averaged ground-state transmission probability assumed by conventional transition-state theory with classical treatment of reaction-coordinate motion—i.e.,

$$\kappa(T) = \frac{\int_0^\infty P(E_{\text{rel}}) \exp(-E_{\text{rel}}/k_B T) dE_{\text{rel}}}{\int_{V_b^{\text{VAG}}}^\infty \exp(-E_{\text{rel}}/k_B(T)) dE_{\text{rel}}}, \quad [4]$$

in which V_b^{VAG} is the ground-state, s -wave vibrationally adiabatic barrier height. Notice that, because of the bending contributions to the vibrationally adiabatic barrier, the transmission coefficient calculated here for the three-dimensional reaction does not equal the one that would be calculated for the collinear reaction. The justifications for considering only the ground-state, s -wave vibrationally adiabatic barrier are as follows. (i) This gives a unified treatment of quantal effects on reaction-coordinate motion which is applicable at both low and high temperatures. At low temperature only the ground state and s -wave contribute; at high temperature $\kappa(T)$ tends to unity whether or not we calculate a thermal average over a sequence of vibrationally adiabatic barriers corresponding to different reactant states. (ii) For the present reaction, excited vibrational states of the reactants make a negligible contribution at 600 K and lower. (iii) For reactant states with nonzero angular momentum, there can be a partial compensation of decreasing rotational energy by increasing bending energy as the system progresses along the reaction coordinate so that approximating the excited vibrationally adiabatic barriers by the ground-state, s -wave one might not be too seriously in error.

We test the dynamical treatment by comparing transition-state theory calculations for the Porter-Karplus potential energy surface no. 2 (17) to the accurate dynamical calculations of Schatz and Kuppermann for this surface. The results are shown in Table 1, in which they are compared to the close coupling distinguishable-atom rate constants of Schatz and Kuppermann (5) for the 100–600 K temperature range. Schatz and Kuppermann did not calculate results at higher temperatures because they performed accurate quantal calculations only up to a total energy of 0.7 eV. This may also contribute to their results being less certain at 600 K. At temperatures below room temperature the calculations are very sensitive to the approximations in the

Table 1. Rate constants ($\text{cm}^3 \text{ molecule}^{-1} \text{ sec}^{-1}$) for Porter-Karplus potential surface no. 2

T, K	Distinguishable atoms			$k_{\text{obs}}^{\text{H}}$ Close coupling†
	Close coupling*	Present calculation	% error	
100	7.71(−21)‡	4.31(−21)	−44	7.34(−21)
200	1.58(−17)	8.02(−18)	−49	1.54(−17)
250	1.70(−16)	1.16(−16)	−32	1.67(−16)
300	9.91(−16)	7.99(−16)	−19	9.80(−16)
400	1.09(−14)	1.05(−14)	−4	1.08(−14)
500	5.00(−14)	5.49(−14)	+10	4.96(−14)
600	1.43(−13)	1.76(−13)	+23	1.42(−13)

* Computed from state-selected distinguishable-atom rate constants (supplied by Schatz from the work reported in ref. 5) by setting all f_j equal in equations 3.6 and 3.7 of ref. 5.

† Computed from table 7 of ref. 5.

‡ In tables, numbers in parentheses are powers of ten.

tunneling correction, and the present results are too low. Schatz and Kuppermann report that their reaction cross sections are converged and satisfy time-reversal symmetry within 5–15%, and they report that two different methods of thermal averaging disagreed by 20%. Thus, the overall uncertainty in their rate constants is at least 25–35%. The present calculations agree with their results within 23% over the 300–600 K temperature range, confirming the accuracy of our methods for these temperatures within this tolerance.

The reliability of the Marcus-Coltrin adiabatic tunneling path is also confirmed by its accuracy for collinear calculations (7, 18). In the collinear case, quantum mechanical rate constants are known within a few percent (19, 20) for both the Porter-Karplus surface no. 2 and the potential surface of Truhlar and Kuppermann (19). The latter surface agrees very well with the *ab initio* calculations of Liu (3) for collinear geometries. By use of results of similar calculations reported elsewhere (18), it is easy to calculate that transition-state theory calculations like the present ones (but for the collinear reaction) are accurate within 25 and 12%, respectively, for these two surfaces at 300 K and are even more accurate at 400–1000 K (21) and for ²H + ²H₂. These successes of the method give confidence that its success for the three-dimensional H + H₂ reaction on Porter-Karplus surface no. 2 is not a fluke. The difficulty of obtaining as good agreement as obtained in Table 1 (error of a factor of 1.2 at 300 K) for thermal rate constants for H + H₂ should be emphasized. Previous transition-state theory calculations with tunneling corrections based on separable reaction coordinates had errors of factors of 2.0–3.4 for the collinear reaction at 300 K (19, 21). Use of the exact collinear transmission probabilities to compute approximate transmission coefficients for the three-dimensional reaction also leads to errors of greater than a factor of 2 at 300 K (22). The nonseparable method of Chapman *et al.* (23) had more success, but still involved errors of 16 and 37% for collinear reaction on the surfaces of refs. 17 and 19, respectively, at 300 K. Another disadvantage of the nonseparable calculations is that they are more difficult than the present calculations; because of this, the only application of the nonseparable method to a three-dimensional reaction involved a 58% sampling uncertainty (23).

The distinguishable-atom rate constants neglect the effect of antisymmetrization of the wave function with respect to protonic coordinates. However, in the classical limit the distinguishable-atom rate constant equals $k_1 + k_{-1}$, which sum is a directly observed quantity $k_{\text{obs}}^{\text{H}}$ in experiments on the consumption of excess *para*-H₂ (1, 24, 25). Calculations actually involving protonic antisymmetrization (5) are also shown in Table 1. They indicate that the distinguishable-atom rate

constant equals $k_1 + k_{-1}$ within 2% or less at 300 K or higher. Thus, in the rest of this article we interpret distinguishable-atom rate constants as calculations of $k_{\text{obs}}^{\text{H}}$. The calculations of Schatz and Kuppermann (5) and the present calculations both neglect the effect of the conical intersection on the antisymmetrization (26). This effect is hard to estimate without full calculations, but it is most important when, from the classical path point of view, there is interference between trajectories passing on opposite sides of the conical intersection (26). Such interference is not expected to play a big role at the temperatures considered here.

The effect of errors of the potential surface can also be estimated. There are several possible ways (2–4) to estimate the basis-set truncation errors in the calculations of Liu and Siegbahn. The calculated classical barrier height is 9.80 kcal/mol. One estimate (2) of approximate bounds on the true classical barrier height is 9.69 ± 0.12 kcal/mol. Errors in the stretching and bending modes are expected to be smaller than the error in the asymmetric stretch mode that contains the barrier. Thus, we scaled the potential energy along the minimum-energy path by 9.57/9.80, retained all stretching and bending force constants unchanged, and repeated the calculations. The results for the scaled surface are shown in Table 2. The percentage change in the calculated rate is 32% or less for 300–600 K. We can also make a comparison to use of the partly semiempirical potential surface of Yates and Lester (27). Whereas the root-mean-square deviation of the analytic fit of ref. 14 from the *ab initio* points of Liu and Siegbahn (3, 4) is 0.09 and 0.23 kcal/mol for linear and nonlinear geometries, respectively, that for the surface of Yates and Lester, which predated ref. 4, is 1.24 and 6.41 kcal/mol, respectively. However, the Yates–Lester surface does have a classical barrier height of 9.82 kcal/mol and a saddle-point-symmetric-stretch frequency and bond length that are accurate within about 1%. The rate constant calculated with their surface is 3.10–1.70 times lower than the present one in the 300–600 K temperature range. At 300 K, a factor of 2.02 comes from the transmission coefficient and a factor of 1.53 comes from the rest of the calculation. Comparison to Table 1 shows that the Porter–Karplus surface no. 2, with a classical barrier height of 9.13 kcal/mol, leads to a calculated rate constant a factor of 4.1–1.8 times larger than that for the surface of ref. 14 in the 300–600 K temperature range. We think that the scaled surface described above provides the most reasonable estimates of possible errors that are caused by the inaccuracies in the surface.

Combining the tests of Tables 1 and 2, we estimate that the overall probable reliability of the present calculation of $k_{\text{obs}}^{\text{H}}$ is about 40–50% at 300–600 K and that calculations with the Porter–Karplus surface no. 2 and the Yates–Lester surface do not have this percentage reliability at temperatures below 1000 K.

Comparison to experiment

There is only one modern experiment on the rate of reaction 1. This is a flow-tube study by Schulz and LeRoy (24) in the temperature range 300–444 K. The experiment directly yields

Table 2. Calculated rate constants $k_{\text{obs}}^{\text{H}}$ ($\text{cm}^3 \text{ molecule}^{-1} \text{ sec}^{-1}$) for three different potential surfaces

T , K	Surface of ref. 14	Scaled surface	% difference	Surface of ref. 27
300	1.95(–16)	2.57(–16)	+32	6.29(–17)
400	3.75(–16)	4.68(–16)	+25	1.69(–15)
500	2.51(–14)	3.02(–14)	+20	1.34(–14)
600	9.51(–14)	1.11(–13)	+17	5.58(–14)
1000	1.77(–12)	1.95(–12)	+10	1.20(–12)

$k_{\text{obs}}^{\text{H}}$, defined above as $k_1 + k_{-1}$, and the authors represented their results by a three-parameter expression which fits all 16 measurements within 7%, thus indicating their precision. Another set of experimental values, which may well be more accurate, can be obtained by combining a measurement (28) of $k_{\text{obs}}^{\text{H}}/k_4$, where reaction 4 is $\text{H} + {}^2\text{H}_2 \rightarrow \text{H}^2\text{H} + {}^2\text{H}$ and Westenberg and deHaas's measurement (29) of k_4 . The ratio was measured in the range 294–693 K with a precision of about 10%, and a least-squares fit to the logarithm of the ratio yields

$$k_{\text{obs}}^{\text{H}}/k_4 = 1.291 \exp(619.9/T), \quad [5]$$

which agrees with all the measurements within their estimated errors. This can be used with the value of k_4 that were measured at five temperatures in this range to yield $k_{\text{obs}}^{\text{H}}$ at five temperatures. k_4 has also been measured by Schulz and LeRoy (30), but we believe from the discussion of Mitchell and LeRoy (31) of the ${}^2\text{H} + \text{H}_2$ reaction that the measurements of Westenberg and deHaas may be more accurate.

The comparison of the present *ab initio* calculations to the experimental values is shown in Table 3. Table 3 also shows values calculated with the scaled potential surface for comparison. Notice that the experimental results do not agree with one another within the sum of their respective 7% and 15–18% precisions. Thus, the systematic errors, which are impossible to estimate, are larger than this sum. A more realistic estimate of the experimental uncertainty in this temperature range is the maximum deviation of the two sets of experimental results, namely, 33%. It is encouraging that in the 327–440 K temperature range the present calculation agrees with the lower experimental result within 24% and with the higher result within 7%. At 549 K, the present calculation is 12% lower than the experimental result. At the lowest temperature, 299 K, the present calculation falls 28% and 29% lower than the experiments, respectively. Thus, our calculation seems to be consistent with the experimental results within the accuracy with which the experimental results are known.

Theoretical comparisons

Table 4 presents additional calculations in which tunneling or both tunneling and anharmonicity are neglected. This allows comparison with some previous transition-state theory calculations (32, 33) using other potential energy surfaces (32–34). First, consider calculations in which tunneling is neglected. These calculations show that the effect of anharmonicity on the surface of ref. 14 is to decrease the rate by a factor of 1.36–1.21 at 300–600 K, and the effect is similar for the Porter–Karplus surface no. 2. The main reason for the difference between the two calculations that neglect tunneling and anharmonicity for the Porter–Karplus potential surface is the vibrationally adiabatic barrier height: the calculations of ref. 32 used H_2 energy levels based on experiment rather than the ones corresponding to the potential energy surface. Other differences between these calculations effect the rate by less than 5%. Next, consider the

Table 3. Calculated and measured rate constants $k_{\text{obs}}^{\text{H}}$ ($\text{cm}^3 \text{ molecule}^{-1} \text{ sec}^{-1}$)

T , K	Calculated		Measured	
	Surface of ref. 14	Scaled surface	Ref. 24	Refs. 28 and 29
299	1.88(–16)	2.48(–16)	2.62(–16)	2.66(–16)
327	5.03(–16)	6.53(–16)	5.17(–16)	5.38(–16)
346	9.10(–16)	1.17(–15)	8.26(–16)	9.77(–16)
440	8.78(–15)	1.08(–14)	7.06(–15)	9.38(–15)
549	5.08(–14)	6.02(–14)	—	5.77(–14)

Table 4. Comparison of calculated values of $k_{\text{obs}}^{\text{H}}$ ($\text{cm}^3 \text{ molecule}^{-1} \text{ sec}^{-1}$)

Anharmonicity?	No	No	Yes	Yes	No	No	No	Yes	Yes
Tunneling?	No	No	No	Yes	No	Yes	No	No	Yes
Surface? ref.	17*	17*	17*	17*	33,34†	33,34†	14‡	14‡	14‡
Ref.	32	Present	Present	Present	33	33	Present	Present	Present
<i>T</i> , K									
250	—	4.97(−20)	2.38(−18)	1.16(−16)	1.57(−18)	2.05(−17)	1.68(−18)	1.17(−18)	2.19(−17)
300	5.00(−17)	6.76(−17)	4.37(−17)	7.99(−16)	3.14(−17)	2.03(−16)	3.33(−17)	2.45(−17)	1.95(−17)
400	1.85(−15)	2.17(−15)	1.65(−15)	1.05(−14)	1.33(−15)	4.12(−15)	1.40(−15)	1.10(−15)	3.75(−15)
500	1.63(−14)	1.86(−14)	1.47(−14)	5.49(−14)	1.27(−14)	2.76(−14)	1.35(−14)	1.09(−14)	2.51(−14)
600	7.14(−14)	7.94(−14)	6.41(−14)	1.75(−13)	5.89(−14)	1.04(−13)	6.24(−14)	5.15(−14)	9.51(−14)
1000	1.60(−12)	1.70(−12)	1.41(−12)	2.30(−12)	1.49(−12)	1.91(−12)	1.60(−12)	1.34(−12)	1.77(−12)

* Porter–Karplus no. 2.

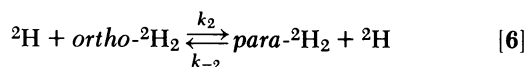
† Surface of ref. 34 scaled in ref. 33.

‡ Fit to *ab initio* points of refs. 3 and 4.

inclusion of tunneling. For the surface of ref. 14, the transmission coefficient is 7.93 at 300 K and 1.85 at 600 K. Thus, both anharmonicity and tunneling are important in this temperature range. Notice that the present calculations are in remarkable agreement with those of Shavitt (33). This is partly fortuitous because he neglected anharmonicity, and the method he used to include tunneling is now known (7, 16, 18, 19, 21) to be unreliable.

Kinetic isotope effect

The sum of the rate constants for the reactions



has also been measured (1, 35) and is called $k_{\text{obs}}^{\text{D}}$. For the temperature range of the modern measurement, 358–468 K, it can be equated with negligible error to the distinguishable-atom rate constant (25). The potential surface is the same as for reaction 1. Using the same methods as for $k_{\text{obs}}^{\text{H}}$, we have calculated $k_{\text{obs}}^{\text{D}}$; the results are in Table 5. The theoretical method is expected to be even more valid for this reaction than for reaction 1 (7, 13). We also computed the kinetic isotope effect—i.e., the ratio $k_{\text{obs}}^{\text{D}}/k_{\text{obs}}^{\text{H}}$. Experimental values for the kinetic isotope effect may be obtained by taking the ratio of the results of refs. 24 and 35. Above 450 K, the Arrhenius plot of k_4 from ref. 29 becomes linear, and we can obtain $k_{\text{obs}}^{\text{D}}/k_{\text{obs}}^{\text{H}}$ by combining the results of refs. 28, 29, and 35. A value for 440 K is also available by combining data from these references. The predicted rate constant and kinetic isotope effect are compared to experiment in Table 5.

In the 368–468 K temperature range, the calculated rate constant $k_{\text{obs}}^{\text{D}}$ is 36–21% lower than the experimental one. Because there is only one experimental measurement, there is no experimental check of the reliability of the measurement. If we assume that the 33% estimate of reliability that we used for the experimental measurements of $k_{\text{obs}}^{\text{H}}$ is also roughly applicable to the experimental measurements of ref. 35, then the agreement with experiment is satisfactory. Shavitt's calculations (33) of $k_{\text{obs}}^{\text{D}}$ led to 7.92×10^{-16} and $3.12 \times 10^{-14} \text{ cm}^3 \text{ molecule}^{-1}$

sec^{-1} at 400 and 600 K, which disagree even more with experiment. He concluded, "At the present time it is difficult to say whether this is due to systematic experimental errors, to inappropriate potential surface parameters, to an inadequate treatment of tunneling, or to some fundamental deficiency of transition-state theory." It is a measure of progress that the reliability of the present calculation is much better documented, and we conclude that our calculated kinetic isotope effect is at least as reliable as the experimental results in this case. It will be a challenge to obtain another measurement of the kinetic isotope effect to try to confirm our prediction.

Concluding remarks

In some respects the $\text{H} + \text{H}_2$ reaction is still unique in the opportunities it presents for *ab initio* calculations of reaction rates. For other cases with even a few more electrons, the electronic structure problems involved in calculating a potential energy surface are sufficiently more difficult that a quantitatively reliable surface is still unavailable (36). The accuracy of the approximate methods for treating the dynamics can be tested definitively only for $\text{H} + \text{H}_2$ because that is the only case for which converged quantal rate constants for a given potential energy surface are available. Converged quantal rate constants for other reactions involving heavier atoms would be more expensive (37). Tests against exact quantal rate constants for collinear reactions on known potential energy surfaces indicate that the Marcus–Coltrin tunneling path is more accurate for the symmetric case with all equal masses than for other cases for which the best tunneling path may be harder to parametrize or the separability assumption may fail (7, 18). The high potential-energy barrier and mass combination of $\text{H} + \text{H}_2$ also tend to make transition-state theory with a dividing surface located at the saddle point more valid than for many other reactions. For reactions with lower barriers, entropy effects can compete with energy effects in determining the location of the dynamical bottleneck to reaction, and variational transition-state theory is often required to find the best generalized transition state (9, 38). There has been much recent progress on techniques for efficient calculations of potential energy

Table 5. Calculated and measured rate constants $k_{\text{obs}}^{\text{D}}$ ($\text{cm}^3 \text{ molecule}^{-1} \text{ sec}^{-1}$) and kinetic isotope effects

<i>T</i> , K	$k_{\text{obs}}^{\text{D}}$		$k_{\text{obs}}^{\text{H}}/k_{\text{obs}}^{\text{D}}$		
	Calculated	Measured ref. 35	Calculated	Measured refs. 24 and 35	Measured refs. 28, 29, and 35
358	2.86(−16)	4.45(−16)	4.50	2.48	—
400	9.48(−16)	1.37(−15)	3.96	2.16	—
440	2.45(−15)	3.29(−15)	3.59	2.15	2.85
468	4.36(−15)	5.54(−15)	3.39	2.24	2.94
600	3.44(−14)	—	2.76	—	—

surfaces and quantal dynamics and methods for variational transition-state theory calculations, but completely *ab initio* calculations of reaction rates with reliability within 50% will be a difficult challenge for most reactions for a long time.

We are grateful to G. C. Schatz for supplying information about and results of the calculations of ref. 5. This work was supported in part by the National Science Foundation under Grant CHE77-27415.

1. Truhlar, D. G. & Wyatt, R. E. (1976) *Annu. Rev. Phys. Chem.* **27**, 1-43.
2. Truhlar, D. G. & Wyatt, R. E. (1977) *Adv. Chem. Phys.* **36**, 141-204.
3. Liu, B. (1973) *J. Chem. Phys.* **58**, 1924-1937.
4. Liu, B. & Siegbahn, P. (1978) *J. Chem. Phys.* **68**, 2457-2465.
5. Schatz, G. C. & Kuppermann, A. (1976) *J. Chem. Phys.* **65**, 4668-4692.
6. Marcus, R. A. & Coltrin, M. E. (1977) *J. Chem. Phys.* **67**, 2609-2613.
7. Garrett, B. C. & Truhlar, D. G. (1979) *J. Phys. Chem.* **83**, 200-203, and erratum in preparation.
8. Garrett, B. C. & Truhlar, D. G. (1979) *J. Phys. Chem.* **83**, 1915-1924.
9. Garrett, B. C. & Truhlar, D. G. (1979) *J. Am. Chem. Soc.* **101**, 4534.
10. Glasstone, S., Laidler, K. J. & Eyring, H. (1941) *The Theory of Rate Processes* (McGraw-Hill, New York).
11. Johnston, H. S. (1966) *Gas Phase Reaction Rate Theory* (Ronald, New York).
12. Weston, R. E. & Schwarz, H. A. (1972) *Chemical Kinetics* (Prentice-Hall, Englewood Cliffs, NJ).
13. Truhlar, D. G. (1979) *J. Phys. Chem.* **83**, 188-198.
14. Truhlar, D. G. & Horowitz, C. J. (1978) *J. Chem. Phys.* **68**, 2466-2476, and erratum (1979) *J. Chem. Phys.* **71**, 1514.
15. Strauss, H. L. & Thiele, E. (1967) *J. Chem. Phys.* **46**, 2473-2480.
16. Truhlar, D. G. & Kuppermann, A. (1971) *J. Am. Chem. Soc.* **93**, 1840-1851.
17. Porter, R. N. & Karplus, M. (1964) *J. Chem. Phys.* **40**, 1105-1115.
18. Garrett, B. C. & Truhlar, D. G. (1979) *J. Phys. Chem.* **79**, 1079-1112.
19. Truhlar, D. G. & Kuppermann, A. (1972) *J. Chem. Phys.* **56**, 2232-2252.
20. Truhlar, D. G., Kuppermann, A. & Dwyer, J. (1977) *Mol. Phys.* **33**, 683-688.
21. Truhlar, D. G. & Kuppermann, A. (1971) *Chem. Phys. Lett.* **9**, 269-272.
22. Kuppermann, A. (1979) *J. Phys. Chem.* **83**, 171-187.
23. Chapman, S., Garrett, B. C. & Miller, W. H. (1975) *J. Chem. Phys.* **63**, 2710-2716.
24. Schultz, W. R. & LeRoy, D. J. (1965) *J. Chem. Phys.* **42**, 3869-3873.
25. Truhlar, D. G. (1976) *J. Chem. Phys.* **65**, 1008-1010.
26. Mead, C. A. & Truhlar, D. G. (1979) *J. Chem. Phys.* **70**, 2284-2296.
27. Yates, A. C. & Lester, W. A. (1974) *Chem. Phys. Lett.* **24**, 305-309.
28. Quickert, K. A. & LeRoy, D. J. (1970) *J. Chem. Phys.* **53**, 1325-1332; and erratum (1971) *J. Chem. Phys.* **54**, 5444-5445.
29. Westenberg, A. A. & deHaas, N. (1967) *J. Chem. Phys.* **47**, 1393-1405.
30. Schulz, W. R. & LeRoy, D. J. (1964) *Can. J. Chem.* **42**, 2480-2487.
31. Mitchell, D. N. & LeRoy, D. J. (1973) *J. Chem. Phys.* **58**, 3449-3453.
32. Karplus, M., Porter, R. N. & Sharma, R. D. (1965) *J. Chem. Phys.* **43**, 3259-3287.
33. Shavitt, I. (1968) *J. Chem. Phys.* **49**, 4048-4056.
34. Shavitt, I., Stevens, R. M., Minn, F. L. & Karplus, M. (1968) *J. Chem. Phys.* **48**, 2700-2713.
35. LeRoy, D. J., Ridley, B. A. & Quickert, K. A. (1968) *Discuss. Faraday Soc.* **44**, 92-107.
36. Ungemach, S. R., Schaefer, H. F. & Liu, B. (1977) *Faraday Discuss. Chem. Soc.* **62**, 330-333.
37. Wyatt, R. E. (1977) in *State-to-State Chemistry*, eds. Brooks, P. R. & Hayes, E. F. (American Chemical Society, Washington, DC), pp. 185-205.
38. Garrett, B. C. & Truhlar, D. G. (1979) *J. Am. Chem. Soc.*, in press.